APOE4 Regulates Synaptic Function by Directly Modulating the SNARE Complex Assembly

Feng Chen
Guangdong Medical University
Yanting Chen
Guangdong Medical University
Huiyi Chen
Guangdong Medical University
Yongxiang Wang
Guangdong Medical University
Wenyan Wei
Guangdong Medical University
Yujie Cai
Guangdong Medical University
Chunmei Liang
Guangdong Medical University
Hao Cao
Shenyang Pharmaceutical University
Xiongjin Chen
Guangdong Medical University
Yao Ji
Guangdong Medical University
Dandan Zhang
Guangdong Medical University
Yuanhong Sun
University of North Texas Health Science Center
Yan Wang
Guangdong Medical University
Lili Cui (cuilili@gdmu.edu.cn)
Guangdong Medical University https://orcid.org/0000-0003-0273-2531

Research article

Keywords: APOE4, SNARE complex, synaptic function

Posted Date: April 9th, 2021

DOI: https://doi.org/10.21203/rs.3.rs-380304/v1

Abstract

Background: The ε4 allele of the Apolipoprotein E (*APOE*) gene is a major genetic risk determinant of sporadic Alzheimer's disease (AD). Its protein product APOE4 has been demonstrated to coffers deleterious effects for various neurodegenerative disorders related to cognitive impairment, including AD. A line of evidence implied that APOE4 affects these diseases partly through its synaptic damage. However, the mechanisms underlying this have not been fully interpreted.

Methods: Proteomics analysis, Co-immunoprecipitation assay (Co-IP), Bimolecular fluorescence complementation (BIFC), and Proximity ligation assay (PLA) assays were used to screen and verify the interactome of APOE, which in an APOE4-priority manner. The molecular docking and molecular dynamic analysis were conducted to elucidate the molecular mechanisms that APOE3 differs from APOE4 in the binding ability of VAMP2. Adeno-associated virus expressing APOE3 and APOE4 was stereotaxically injected into the Hippocampus of *Apoe-/-* mice, and *in vitro* recombinant proteins experiments were conducted to verify the AOPE on soluble N-ethylmaleimide-sensitive factor attachment protein receptor (SNARE) complex assemble. FM4-64 fluorescent dye labeling assay was explored in hippocampus from APOE3-TR and APOE4-TR mice to study the APOE genotype effect on synaptic vesicle release**.**

Results:

Using proteomics analysis, we screened interactomes of APOE3 and APOE4 in neurons, respectively. Then, VAMP2 protein was selected for further analysis through related bioinformatics analysis. Via Co-IP, BIFC, and PLA assays,we demonstrated that APOE directly interacts with VAMP2 in an E4 > E3 manner *in vitro* and *in vivo*. The molecular docking and molecular dynamic analysis suggested that the APOE4-VAMP2 complex was more stable and had higher affinity than APOE3-VAMP2, may due to the increased contribution of hydrogen bonding, hamper VAMP2 to form the SNARE complex. The further in vitro and in vivo results suggest that APOE4 blocks the SNARE complex assembly, negatively regulating synaptic vesicle release, finally contributing to the synaptic damage and cognitive impairment.

Conclusions:

Our findings identify SNARE protein as an APOE interactor, and APOE4 isoform effects on SNARE complex formation, mediates APOE4-induced synaptic dysfunction. Our results provide insights into APOE4-mediated synapse toxicity, and suggested new avenues for specifically targeting early presynaptic dysfunction in AD.

Background

Alzheimer’s disease (AD), which is the most common type of neurodegenerative disease and a leading cause of mortality in the elderly [1], is characterized by the pathological accumulation of amyloid-β (Aβ) plaques and neurofibrillary tangles, along with progressive memory loss and synaptic alterations in the brain [2]. Among the distinctive neuropathological hallmarks of AD, the extent of synaptic loss has been

reported as the best pathological correlate of cognitive decline and memory deficits [3-6]. Increasing evidences highlights that presynaptic dysfunction might be an early event that occurs before neurodegeneration and interfering with early synaptic dysfunction may be therapeutically beneficial in preventing cognitive decline and disease progression [7, 8]. However, the molecular mechanisms underlying such synaptic failure remain largely unknown.

Clinical studies, along with basic research, have widely demonstrated that the ε4 allele of the *APOE* gene is the strongest genetic risk factor for late-onset AD with an earlier stage of the disease developing in a gene dose-dependent manner relative to the risk-neutral ε3 allele [9, 10]. Indeed, carrying one copy of the ε4 allele increases the risk of AD by about 3-fold, with homozygotes having a 12-fold higher susceptibility to develop AD, making it the most significant risk gene for sporadic AD [11, 12]. In addition to AD, APOE4 is also a genetic risk factor for a variety of neurodegenerative disorders related to cognitive impairment, such as Parkinson's disease dementia, frontotemporal dementia, Lewy body dementia and cerebrovascular disease [13-16]. Human APOE3 and APOE4 differ from each other only at one amino acid residue at position 112. The single amino acid difference between APOE3 (Cys112) and APOE4 (Arg112) has been shown to substantially alter the structure and function of APOE proteins, such as binding to apolipoprotein receptors, lipids, and Aβ [17-20]. Despite the substantial influence of APOE4 on the progression of AD, how APOE4 modulates the molecular mechanisms underlying neurodegeneration remains elusive.

As the major lipid transport protein in the central nervous system (CNS), APOE has many functions such as immunomodulation, signal transduction, and maintenance of synaptic connections [21-23]. It has been reported that APOE4 was negatively associated with dendritic spine density of dental gyrus neurons in both aged normal controls and patients with AD [24, 25]. In addition, animal studies have reported that APOE4-targeted replacement (TR) mice have less dendritic arborization and reduced synaptic transmission compared to APOE3-TR mice, and that these reductions occurred in the absence of any pathologic hallmarks such as gliosis, amyloid deposition, or neurofibrillary tangles [26, 27]. These findings highlight a key role of APOE4 in perturbing synaptic function in early disease stages, may be an independent risk factor for synapse loss and neurodegeneration. Although increasing data imply the involvement of APOE in synaptic regulation, its molecular mechanism remains poorly investigated.

Synaptic transmission relies on the fusion of synaptic vesicles with the presynaptic plasma membrane. In presynaptic terminals, neurotransmitter secretion requires a tightly coordinated membrane fusion machinery with the soluble N-ethylmaleimide-sensitive factor attachment protein receptor (SNARE) [28, 29]. At synapses, neuronal SNARE proteins mainly comprise the vesicle-associated SNARE (v-SNARE) protein VAMP2 (also referred to as synaptobrevin-2) and the plasma membrane t-SNARE proteins, syntaxin-1 and SNAP25 [30]. Aberration in SNARE complex formation is highly associated with cognitive function [31, 32], and it has been suggested that misfolded proteins cause cognitive impairments in relation to neurodegeneration by impairing presynaptic chaperones or directly inhibiting SNARE complex formation [33, 34]. In particular, the ability of SNARE proteins to form complexes was found to be a predictor of cognitive function [35]. Analysis of these presynaptic proteins suggests that the level of their

functional interactions is associated with greater brain reserve, better cognition, and less decline over time [7, 36]. Importantly, investigations indicate that the formation of the SNARE complex is substantially decreased in the postmortem brains of AD and PD patients as well as the AD mouse model [37, 38], and maintaining the SNARE complex function in neurotransmission is important to prevent neurodegeneration. As an important risk gene for neurodegenerative diseases and cognitive impairment, the mechanism underlines the correlation between different APOE genotypes and SNARE remains largely unknown and whether APOE can affect the assembly of SNARE needs further interrogated. In the present study, we investigated the potential contribution of the APOE4 genotype to dementia-related pathogenesis by directly binding and downregulating the SNARE complex assembly.

Materials And Methods

Animals

C57BL/6J and APOE knockout mice were purchased from The Jackson Laboratory. Human APOE3- and APOE4-TR mice were purchased from Cyagen Biosciences. Mice were maintained at a controlled temperature of 24–26°C under a 12-h light/dark cycle. The mice had free access to food and purified water. All animal experimental procedures were performed in accordance with the Guide for the Care and Use of Laboratory Animals and approved by the Laboratory Animal Ethical Committee of Guangdong Medical University. Female mice were selected because previous work has shown that behavioral and molecular deficits in APOE4-TR mice are more pronounced in female mice, consistent with observations in humans showing higher risk for AD in female APOE4 carriers.

Primary neuronal culture and mass spectrometry

Primary hippocampal or cortical neurons were obtained from newborn APOE knockout mice. Cultures were grown in a neurobasal medium supplemented with B27 (Thermo Fisher Scientific), 0.5 mM glutamine, 100 U/mL penicillin, and 100 g/mL streptomycin. Neurons were seeded at a density of 10^5 cells/well in 6-well plates. At 2 days *in vitro* (DIV), cells were treated with cytosine arabinofuranoside (Ara-C, Sigma) to eliminate glial cells. At DIV7, cells were treated with recombinant human APOE3 (rh-APOE3; PeproTech, Lot: 06188) and APOE4 (rh-APOE4; PeproTech, Lot: 0118318) for 24 h at 10 μM before cells were harvested. The cells were lysed and incubated with APOE (ab1906) or IgG antibodies overnight at 4°C, followed by treatment with protein A/G PLUS-Agarose (GE Healthcare, Lot: 10247533 and 10248260) for 2 h. Then, the protein complexes were washed three times with the immunoprecipitation (IP) buffer and boiled for 3 min, followed by MS analysis. MS was conducted as described previously [39]. Briefly, total proteins were extracted from cells using IP lysis buffer (20 mM Tris-HCl pH 7.5, 150 mM NaCl, 1% Triton X-100, 1 mM EDTA, 5% glycerol; Beyotime, P0013). The relevant antibodies and protein A/G beads were added to the protein lysates. Next, the lysates were incubated at 4°C overnight. Pre-cold IP lysis buffer was used to wash the immunocomplex samples three times. Lastly, the samples were boiled in SDS-PAGE loading buffer and analyzed by western blotting.

Co-immunoprecipitation assay

For Co-IP analysis, HEK-293T cells were co-transfected with pCMV-VAMP2-HA and pCMV-APOE3-3 × Flag or pCMV-APOE4 × 3Flag plasmids. After 48 h of transfection, the cells were washed with PBS and lysed with IP lysis buffer for 30 min at 4°C. The supernatant of cell lysates was incubated with the respective antibodies overnight at 4°C, followed by treatment with protein A/G PLUS-Agarose for 2 h at 4°C. Beads were washed three times with lysis buffer before suspension in an equal volume of 2× SDS sample buffer. Protein bands were detected by western blotting using the anti-Flag (Abbkine, A02010) and anti-HA (Abbkine, A02040) antibodies.

Western blotting

The antibodies and recombinant proteins used in this study are listed in Table S1(Additional file1). Mouse brain tissues and cultured cells were homogenized and lysed in RIPA buffer (20 mM Tris-HCl [pH 7.5], 150 mM NaCl, 1 mM EGTA, 1 mM EDTA, 1% Triton X-100, 1% sodium deoxycholate, 1 mM PMSF, 10 mg/mL aprotinin, 1 mg/mL pepstatin A, and 1 mg/mL leupeptin). The proteins were then quantified using the Pierce™ BCA Protein Assay Kit (Thermo Fisher Scientific, TL276863). Equal amounts of protein were resolved by SDS-PAGE and transferred to polyvinylidene fluoride membranes. After the membranes were blocked, proteins were immunoblotted with a relative primary antibody, followed by secondary IgG antibodies conjugated with horseradish peroxidase. Finally, the blots were visualized by enhanced chemiluminescence. To study SNARE complex formation, the protein concentration of each lysate was determined, and the samples from each genotype were then divided into two tubes: one tube was boiled for 30 min, and the other was kept at 24°C.

Bimolecular fluorescence complementation assay

Due to stronger complementation signals and direct readout, the BiFC assay has been widely accepted and used for the study of protein-protein interactions in living cells. For the BiFC assay, cDNAs coding for APOE3 and APOE4 were subcloned into a FLAG-tagged C-terminal Venus vector (pBiFC/Flag-VC155), and VAMP2 was subcloned into an HA-tagged N-terminal Venus plasmid (pBiFC/HA-VN173). VC and VN are the C-terminal and N-terminal fragments of the Venus fluorescent protein, respectively. HEK-293T cells were co-transfected with cloned BiFC vectors (APOE-VC with VAMP2-VN or APOE-VC with VN-VAMP2) using Lipofectamine 2000 (Invitrogen, 11668019) according to the manufacturer's protocol. After 48 h of transfection, Venus fluorescence signals were imaged using a confocal microscope (Olympus, Tokyo, Japan).

Molecular docking and molecular dynamics simulation

MDS is one of the most useful techniques that provides the possibility of studying the stability of biological macromolecules and monitoring their behavior over time. The crystal structure of APOE3 was obtained from the Protein Data Bank (PDB ID: 2l7b). The 112-position Cys residues of APOE3 protein were mutated to Arg as the initial structure of APOE4 by PyMOL 2.1. Then, 20 ns molecular dynamics

simulation of the APOE4 protein was performed using the GROMACS software, and the final equilibrium structure was used for docking with the VAMP2 protein. Since there is a complete crystal structure of the VAMP2 protein, homologous modeling is needed to construct its complete structure. Modeler 9.24 software was used for single template modeling, Swiss model was used for template search, and PDB ID: 3hd7 was selected as the template for modeling. The homology and resolution were 100% and 3.4%, respectively. The Rosetta software was used to optimize the structure, and SAVE V5.0 was used to evaluate the protein quality. The online server swarm docking server connects APOE3, APOE4, and VAMP2. The docking type was blind docking, and the number of generated models was set to 200. Finally, according to the docking score, the optimal complex conformation was selected as the initial structure of MDS. MDS was performed under constant temperature, constant pressure, and periodic boundary conditions using the GROMACS program. In the MDS process, all hydrogen bonds were constrained by the LINCS algorithm, and the integration step was 2 fs. The electrostatic interaction was calculated using the particle-mesh Ewald method, and the cutoff value was 1.2 nm. The non-key interaction truncation value was set to 10 Å and updated every 10 steps. The V-rescale temperature coupling method was used to control the simulation temperature of 300 K, and the Berendsen method was used to control the pressure of 1 bar. Different systems of APOE3-VAMP2 and APOE4-VAMP2 were simulated by MD at 100 ns, and the conformation was saved every 10 ps. The binding free energies of APOE3 and APOE4 with the VAMP2 protein were calculated using the MMPBSA program.

Immunofluorescence staining

The mice were perfused with PBS, followed by 4% paraformaldehyde. After fixation, whole brains were dissected and embedded in OCT compound. Coronal brain sections (10 μm) were fixed with 4% paraformaldehyde and blocked with 1% goat serum albumin containing 0.3% Triton for 1 h at room temperature. Then, the slices were incubated with primary antibodies overnight at 4°C. Sections were subsequently washed with PBS and incubated with fluorescent secondary antibodies (Alexa Fluor® 488, 1: 500, Abcam; Alexa Fluor® 647, 1: 500, Abcam) for 2 h at room temperature. Next, the sections were incubated with DAPI (1:1000, Boster) for 5 min to stain the nuclei. Finally, the slides were cover-slipped with mounting medium. Immunofluorescence images were acquired using a confocal microscope (FV3000; Olympus).

Hippocampal stereotactic injections

The AAV-CMV-EGFP, AAV-APOE3, and AAV-APOE4 preparation (2 μL, 1.0×10^{12} IU/mL) was bilaterally injected into the hippocampal CA1 region using a 33-gauge needle (Hamilton) and a syringe pump (KD Scientific, Holliston, MA) at a rate of 0.2 uL/min. Female *APOE*$^{-/-}$ mice were anesthetized with 5% chloral hydrate (8 μL/g), head fur was clipped, and animal heads were fixed on a stereotactic frame. The scalp was disinfected using three separate antiseptic swabs. Erythromycin was used to keep the eyes moist. The head of each mouse was shaved and fixed using a stereotaxic instrument. Following a scalp midline incision, the soft tissues were reflected, and a 5 mm × 5 mm craniotomy was performed between the bregma and lambda (to the left of the sagittal suture) to expose the underlying dura. Stereotactic

coordinates used for injections were as follows: antero/posterior = -2.5 mm, medio/lateral = ±1.8 mm, and dorso/ventral = -2.0 mm coordinates from bregma. After injection, the needle was retained for an additional 2 min before it was slowly withdrawn. After surgery, the scalp was closed with sutures, and the animals were placed in cages and allowed to recover from anesthesia. One month after the injection, mice were sacrificed, and the hippocampal lysates were used for western blot analysis.

Analysis of the SNARE complex

Biochemical analysis of the SNARE complex was performed as previously described, with some modifications. HEK-293T cells were co-transfected with pCDNA-syntaxin-1, VAMP2, and SNAP25 (1:1:1) together with increasing amounts of the APOE3 or APOE4 plasmid. Total DNA was kept constant by balancing the APOE plasmid with an empty plasmid. SH-SY5Y cells and *APOE*$^{-/-}$ primary neurons were infected with AV-APOE3, AV-APOE4, or control adenovirus. Then, 48 hours after transfection or infection, cells were homogenized with lysis buffer (50 mM Tris-HCl (pH 7.4), 150 mM NaCl, 1% NP-40, 0.5% Triton X-100) plus protease inhibitors and centrifuged at 12,000 × g at 4°C for 10 min. The supernatant was mixed with SDS-sample buffer and divided into two fractions. One fraction was boiled for 30 min, while the other was not. Both fractions were subjected to SDS-PAGE and western blot analyses. SDS-resistant SNARE complexes were defined as immunoreactive materials above 40 kDa that were absent from the boiled samples.

In vitro assembly of neuronal SNARE complexes

Recombinant syntaxin-1 proteins (3 mM) were incubated with SNAP25 (3 mM) at room temperature for 2 h to form t-SNARE complexes. Concurrently, recombinant VAMP2 proteins (3 mM) were incubated with recombinant human APOE3 or APOE4 protein (3 mM) at room temperature. SNARE complex formation was initiated by the addition of the above proteins and stopped after 2 h by the addition of SDS-containing sample buffer. The assembly of SNARE complexes was analyzed by SDS-PAGE and Coomassie Brilliant Blue staining. The intensities of the bands corresponding to the tertiary SNARE complex were quantified using a densitometer (GS-900, Bio-Rad).

Proximity ligation assay

PLA was performed using the Duolink *in situ* Red Starter Kit Mouse/Rabbit (Sigma-Aldrich, F1635) following the manufacturer's instructions. Briefly, after washing, permeabilizing, and blocking as histological analysis, cerebral coronal sections were incubated with anti-APOE (ab1906) and anti-VAMP2 (ab181869) primary antibodies overnight at 4°C. The slides were then incubated with anti-mouse MINUS and anti-rabbit PLUS proximity probes for 1 h at 37°C. Ligation and amplification were performed using the Duolink *in situ* detection reagent kit according to the manufacturer's protocol. Finally, the hippocampal CA1 region was mounted on a slide with the Duolink *in situ* mounting medium with DAPI. Images were captured in the hippocampal CA1 region using an Olympus FV1000 confocal microscope, and the red spots represent the interactions between APOE and VAMP2.

FM4-64 fluorescent dye evaluation

SH-SY5Y cells were infected with AV-APOE3, AV-APOE4 or control adenovirus for two days, the cells were incubated with FM4-64 fluorescent dye (Biotium, USA) for 3 min at room temperature to allow the FM4-64 dye to bind to the outer membrane of cells. Next, 70 mM KCl was added to the cells for 3 min to internalize the FM4-64 dye via endocytosis. The cells were then washed with 0.9% NaCl to remove extracellular FM4-64 dye. Then, 70 mM KCl was added again to eliminate synaptic vesicle exocytosis. The FM4-64 fluorescent intensity signal was immediately imaged by confocal microscopy (Olympus, Tokyo, Japan) using a 60× objective lens and a 543 nm argon laser, and images were acquired every 1s for 1 min.

Transmission electron microscopy (TEM)

Female APOE-TR mice (6 months old) were anesthetized with 5% chloral hydrate and perfused with saline, followed by 2% paraformaldehyde in 0.1 phosphate saline (PBS; pH 7.4). Brains were dissected and removed from the skulls quickly and carefully and immersed in the same fixative overnight at 4°C. After washing with 0.1 M phosphate buffer, the CA1 region of the hippocampal tissue was cut into small pieces (1×1×1 mm) and fixed with 2% glutaraldehyde at 4°C for 2 days. Next, tissues were post-fixed with 1% osmium tetroxide for 2 h. Tissues were cut into 70 nm thick sections and stained with uranyl acetate for 30 min and lead citrate for 10 min; the sections were observed under TEM (JEM-1400PLUS). Synaptic ultrastructure including synapse number, synapse size, and length of the active zone were chosen based on a systematic random sampling principle and photographed at a TEM magnification of 60,000×. The small synaptic vesicles were divided into two groups to count as “docked” vesicles (i.e., located within 30 nm of the presynaptic active zone). Finally, the synapse number, synapse size, and active zone length were measured using the ImageJ software.

Statistical analysis

Data are expressed as means ± standard error of the mean (SEM). Student's t test was used to analyze the differences between two groups, one-way ANOVA was used to analyze the differences more than two groups with one independent variable, and two-way ANOVA was used for groups with two independent variables. All the experiments are performed independently at least three times. All data and figures in this paper were analyzed and plotted by GraphPad Prism version 6.0. Statistical significance was set at $P < 0.05$ (*$P < 0.05$, **$P < 0.01$, and ***$P < 0.001$).

Results

In vitro characterization of the different interactions of the APOE genotype

To investigate how the APOE genotype differentially regulates the neuronal function, *Apoe*$^{-/-}$ primary neurons were incubated either with recombinant human APOE3 or APOE4 protein, followed by co-immunoprecipitation (Co-IP) assay and mass spectrometry (MS) analysis to compare the different

interaction proteins between the APOE3 and APOE4 (Fig. 1A). A proteomic analysis identified 1137, 834, and 488 proteins in the APOE3, APOE4, and IgG groups, respectively. Some of these proteins have been previously reported to interact with APOE, for example the microtubule-associated protein [40], suggesting the effectiveness of the proteomic analysis. Among these potential interactions, 324 candidate proteins were unique to the APOE3 group (Additional file2: Table S2), 91 proteins specifically interacted with the APOE4 group (Additional file3: Table S3), and 737 proteins overlapped between them (Fig. 1B). The top five APOE4-specifically enriched proteins (dgcr6, VAMP2, VAMP3, marcks, and krt76) were listed according to their abundance in the MS data. Notably, among these proteins, VAMP2 was identified to be closely related to synaptic transmission [41, 42] and correlated well with the pathological features of AD [43, 44]. Additionally, VAMP2 is one of the main components of the SNARE complex, which is critical for neurotransmission. Furthermore, GO and KEGG analyses also showed that the difference between APOE4- and APOE3-specific interactome was enriched in proteins related to SNARE interactions in the vesicular transport and synaptic vesicle cycle (Fig. 1C and D, Additional file4: Fig. S1A–E). Therefore, VAMP2 protein was selected for further analysis.

Next, the expression of individual SNARE proteins (VAMP2, SNAP25, and syntaxin-1) and SNARE complex in an AD mouse model were investigated. As shown in Fig. S2A (Additional file5), the VAMP2 protein was significantly decreased in the cortex and hippocampus homogenates of APP/PS1 transgenic (TG) mice. The SDS-resistant property of the SNARE complex allowed us to determine the amount of complex formation using SDS-PAGE and western blot analysis. VAMP2 and SNAP25 antibodies were used to individually quantify the amount of the SNARE complex in the cortex and hippocampus homogenates of APP/PS1 TG and wild-type mice. The results showed an approximately 30% decrease in SNARE complex formation in APP/PS1 TG mice (Additional file5: Fig. S2B). These results indicate that SNARE complex assembly was decreased in the AD mouse model.

Interaction of APOE with SNARE proteins in an E4 > E3 manner

Co-IP was performed to confirm the interactions between APOE and VAMP2 proteins in HEK-293T cells. Results showed that APOE co-immunoprecipitated with VAMP2 with higher affinity for APOE4 (Fig. 2A), and vice versa (Fig. 2B), indicating the isoform-dependent binding of APOE and VAMP2 protein. Furthermore, the biomolecular fluorescence complementation (BiFC) assay was performed to validate the interaction between APOE and VAMP2 at the cellular level, which enables the visualization of protein-protein interactions in living cells [45]. In this assay, two candidate interacting proteins were fused to the C- and N-terminal non-fluorescent fragments of the Venus fluorescent protein (VC155 and VN173, respectively). If they interact with each other, the VN173 and VC155 fragments are brought into proximity and produce a fluorescent signal. Our results showed that the co-transfection of VC-APOE4 and VN-VAMP2 or VC-APOE4 and VAMP2-VN plasmids yielded more intense Venus signals (i.e., green fluorescence) than that of APOE3 (Fig. 2C and D) in HEK-293T cells. No fluorescence was detected when APOE or VAMP2 was expressed alone. These results suggest that APOE interacts with VAMP2 in an E4 > E3 manner in living cells. As APOE3 and APOE4 differ only at the single amino acid in position 122, we examined whether APOE (1–136) was responsible for the different interactions (Fig. 2E). As shown in Fig.

2F, APOE4 (1–136) has a higher binding affinity with VAMP2 than APOE3 (1–136), indicating that a single amino acid may contribute to the binding difference. In the CNS, VAMP2 together with SNAP25 and syntaxin-1 constitute the core component of the SNARE complex, which corresponds to the minimal component of the protein machinery that promotes synaptic vesicle fusion with the presynaptic membrane, thereby releasing neurotransmitters. We further determined whether APOE interacts with SNAP25 and syntaxin-1, and the results indicated that APOE co-immunoprecipitated with SNAP25 (Fig. 2G) and syntaxin-1 (Fig. 2I) in an E4 > E3 manner, and vice versa (Fig. 2H and J). These results demonstrated that APOE interacts with the SNARE complex in an isoform-specific manner (E4 > E3).

Binding mechanisms of APOE with VAMP2

Structural bioinformatics and molecular dynamic simulations (MDS) were performed to determine the interactions between the APOE genotype and VAMP2 protein. The stability of the APOE-VAMP2 complexes and their structural changes were examined using the root-mean-square deviation (RMSD), which indicates the average distance between the backbone atoms of superimposed proteins. As shown in Fig. 3A, the RMSD values were similar at the beginning of the simulation (0–20 ns), which was mainly due to the large protein structure fluctuation caused by the interaction between the protein and the surrounding water solvent. The RMSD parameter sharply increased and remained stable with minor residue fluctuations after 50 ns of simulation. The mean RMSD value of APOE4-VAMP2 complex was 2.07 nm with a 1.16% amplitude of fluctuation. Meanwhile, the RMSD value of the APOE3-VAMP2 complex was 2.44 nm, and the fluctuation amplitude was 4.06%. The lower RMSD value of the APOE4-VAMP2 complex in the simulation process indicates that the protein complex is more stable than the APOE3-VAMP2 complex. The radius of gyration (Rg) provides insight into the measure of protein compactness. Therefore, Rg analysis was conducted to further characterize the conformational changes in the APOE-VAMP2 complex structure. As shown in Fig. 3B, the Rg values of the two complexes decreased gradually in the first 20 ns of the simulation, which was mainly due to the longer α-helix of VAMP2 gradually approaching the APOE protein during simulation, and the structure of the two systems became more compact. The average Rg values of APOE3-VAMP2 and APOE4-VAMP2 complex are 2.50 nm and 2.38 nm, respectively. The Rg values of the APOE4-VAMP2 system are relatively smaller, indicating that VAMP2 and APOE4 form frontal complex structures more closely than APOE3; thus, it is speculated that the interaction may be stronger. Hydrogen bonding is an important force for maintaining the structural stability of biological macromolecules, and it is also an important form of protein interaction. Therefore, the number of hydrogen bonds between VAMP2 and APOE proteins during MDS was statistically analyzed. As shown in Fig. 3C, the number of hydrogen bonds between APOE4 and VAMP2 is higher than that of APOE3, with an average of 16.74% and 12.20%, respectively. To further evaluate the difference in affinity between proteins, the free binding energy of APOE3 and APOE4 proteins interacting with VAMP2 during simulation was evaluated. The free binding energy of the APOE protein interacting with VAMP2 was basically stable after 60 ns, and the average binding energy of APOE3 and APOE4 with VAMP2 is −481.21 kJ/mol and −568.57 kJ/mol, respectively (Fig. 3D). These results suggest that the hydrogen bonding interaction and binding energy between APOE4 and VAMP2 were lower than those between APOE3 and VAMP2. APOE3 and APOE4 differ from each other only at one amino acid

residue at position 112, which has been shown to substantially alter the structure and function of the APOE protein. To further study the difference in binding with VAMP2 caused by amino acid mutation at position 112, the amino acid conformation near position 112 of the APOE protein after MDS was analyzed. Detailed analysis of the intermolecular interactions showed that the Cys112 side chain does not play an obvious role in the binding of APOE3 and VAMP2. The binding free energy of APOE3 and VAMP2 mainly depend on the hydrogen bonding between Asp110 and Lys91, Val185, and Asn92, and the hydrophobic interaction between Val116, Val185 (APOE3), and Leu99, Ile98, Met96, Met95, Leu93 (VAMP2) (Fig. 3E). In the binding mode of APOE4 and VAMP2, the side chain of Arg112 turned towards the VAMP2 protein, formed hydrogen bonds with Glu109, and formed cation-π interactions with Tyr88, which is an aromatic amino acid in the VAMP2 structure (Fig. 3F). The distance between Arg112 and the aromatic benzene ring centroid was 4.22 Å. In addition, Arg189 in APOE4 also forms cation-π interactions with Trp89 of VAMP2, and hydrogen bonding interactions exist between the Arg189 main chain and Asn92, Glu238, and Lys91, which further enhances the binding affinity between APOE4 and VAMP2. To further study the difference in APOE genotype binding with VAMP2 protein, the binding modes of APOE and VAMP2 proteins were analyzed. The VAMP2 protein mainly relies on the α-helix structure and binds to the hydrophilic groove of the APOE protein (Fig. 3G and Additional file 6 to 8: Movies S1 to S3). Therefore, it can be inferred that hydrophilic interactions are one of the key forces in the molecular recognition process. Furthermore, there are some hydrophobic regions near the binding surface of the VAMP2 and APOE proteins, and hydrophobic interactions can further enhance protein binding. The VAMP2 regions (31–91) responsible for SNARE complex formation can completely bind to APOE protein, thus hampering SNARE complex assembly by overlapping the VAMP2 structural binding epitope.

Inhibition of the SDS-resistant SNARE complex formation by APOE4 *in vitro* and *in vivo*

The above results showed the APOE genotype-dependent interactions with individual SNARE complexes (VAMP2, SNAP25, and syntaxin-1), indicating that it may inhibit the assembly of neuronal SNARE complexes. To test this hypothesis, we detected the APOE genotype on SNARE complex formation in HEK-293T cells, and the results showed that the overexpression of the APOE4 plasmid significantly inhibited SNARE complex formation as compared with that of the APOE3 plasmid (Fig. 4A). Next, we examined the effect of the APOE genotype on SNARE complex assembly in neuronal cells. The efficacy of adenovirus (AV) infection was confirmed by visualizing the green fluorescent protein (GFP) (Additional file9: Fig. S3A). Consistently, the infection of AV-APOE4 in cultured SH-SY5Y cells (Fig. 4B) and *APOE*$^{-/-}$ primary neurons (Fig. 4C) resulted in a corresponding decrease in SNARE complex assembly, whereas there were no apparent variations in the individual amounts of VAMP2, SNAP25, and syntaxin-1 proteins (Additional file9: Fig. S3B). Because the effect in cultured cells may have been indirect, we examined the function of APOE in a purely *in vitro* system. The syntaxin-1 recombinant protein was incubated with SNAP25 to form t-SNARE complexes, and the VAMP2 recombinant protein was incubated with recombinant human APOE3 or APOE4 protein, then the SNARE complex formation was initiated by the addition of the above proteins and stopped by the addition of SDS-containing sample buffer. The addition of APOE4 resulted in significantly reduced SNARE assembly, as observed by gel band densitometry (Fig. 4D). In addition, we

observed a linear relationship between the SNARE complex assembly and APOE4 levels (Fig. 4E). To test if the *in vitro* results are indicative of the *in vivo* results, one month following the hippocampal injection of the adeno-associated virus (AAV) in 6-month-old *Apoe*$^{-/-}$ mice, GFP was visualized to determine the effect of the injection (Fig. 4F). We observed that SNARE complex formation was significantly decreased in AAV-APOE4-EGFP-injected mice (Fig. 4G).

Decrease in SNARE complex assembly by APOE4 under physiological conditions

To address whether the APOE4-mediated decrease in the SNARE complex assembly is relevant under physiological conditions, APOE-TR mice were chosen to examine the APOE genotype on SNARE complex formation. The endogenous interactions between APOE and VAMP2 were evaluated. Immunofluorescence showed that APOE was co-localized with VAMP2 in the hippocampus of APOE-TR mice (Fig. 5A). Co-IP was performed to confirm the interactions between APOE and VAMP2 proteins in the hippocampus of APOE-TR mice. The results indicated that APOE co-immunoprecipitated with VAMP2 with a higher affinity for APOE4 (Fig. 5B). Additionally, the Duolink assay was performed to confirm the direct interaction between APOE and VAMP2. The Duolink assay is an *in situ* proximity ligation assay (PLA) technology that enables the detection and visualization of direct protein interactions in cell and tissue samples. As shown in Fig. 5C, the Duolink puncta (red) in the hippocampal region of APOE4-TR mice was more obvious than that of APOE3-TR mice, indicating a higher interaction between APOE4 and VAMP2 than APOE3 and VAMP2 *in vivo*. Furthermore, consistent with our *in vitro* data, APOE4-TR mice exhibited decreased SNARE complex assembly in both the cortex and hippocampus (Fig. 5D). Moreover, there was no significant change in the individual SNARE proteins, as determined by western blot and immunofluorescence analysis (Fig. 5E, F and Additional file10: Fig. S4A-C). In summary, the APOE4 genotype directly interacts with the VAMP2 protein and is associated with decreased SNARE complex formation *in vitro* and *in vivo*.

Association of APOE4 with decreased synaptic vesicle release

The effect of the APOE genotype on synaptic vesicle release was determined by the FM4-64 fluorescent dye labeling assay (Fig. 6A), which is widely used to monitor vesicle release in cultured neuronal cells. The F/F0 ratio was reduced to about 0.7 at 10 s and was decreased further to about 0.5 at 30 s. However, the APOE4 markedly blocked the fast-declining fluorescent signal of the boutons with the F/F0 ratio as high as 0.9 at 10 s and 0.7 at 30 s after KCl stimulation (Fig. 6B and Additional file 8,11,12: Movies S3 to S5). Furthermore, the synaptic ultrastructure in the CA1 region of the hippocampus from APOE3-TR mice was assessed. As shown in Fig. 6C, the number and size of synaptic vesicles in each synapse were not altered in either group. However, we observed a significantly lower number of docked vesicles in sections from APOE4-TR mice than in APOE3-TR mice. These results suggest that the reduced synaptic vesicle release by APOE4 may be explained by the docking defect. Overall, the *in vitro* and *in vivo* data provide evidence that APOE4 impairs presynaptic vesicle release.

Discussion

APOE4 variant is the strongest genetic risk factor for later onset of AD and was shown to affect the disease in part through its synaptic damage, which is characterized by diminished neurotransmitter release [26, 46]. However, the mechanism of APOE4-mediated synapse toxicity is still unclear. In the present work, we investigate the molecular mechanisms by which synaptic transmission is affected by APOE4, and raise the possibility that the APOE4 inhibits neurotransmitter exocytosis by directly binding to the SNARE motif, thus inhibit the SNARE complex formation (Figure 7).

AD is a highly prevalent neurodegenerative disorder with a complex and unclear pathogenesis that is characterized by cognitive decline. Synaptic damage and loss are thought to be the earliest pathological change in AD, and most directly correlated with cognitive deficits. In the brain, APOE is primarily secreted by astrocytes and delivers APOE-containing lipoprotein particles to neurons via receptor-mediated endocytosis to support synaptogenesis and maintenance of synaptic connections[47]. APOE4 is less efficient than APOE3 in delivering cholesterol for maintenance of synaptic integrity and plasticity, which may cause a cumulative effect eventually results in synaptic damage and cognitive disorders over an individual's lifetime. This may explain that APOE4 is associated with cognitive decline many years before cognitive impairment becomes clinically apparent[48]. In AD subjects and transgenic mice models, APOE4 displays a gene dose effect in reducing presynaptic protein expression and dendritic spine density[24, 25, 49]. The cognitive deficits are present in APOE4 carries decades prior to any defined neuropathology[50, 51]. In addition, human APOE4 knock-in mice have reduced long-term potentiation in the dentate gyrus compared with APOE3 mice, without evidence of advanced neurodegeneration[52]. Besides, APOE4-TR mice displayed reduced excitatory synaptic transmission and dendritic arborization in the amygdala, without obvious amyloid deposition or neurofibrillary tangles in these mice[26]. Additionally, the presence of the APOE4 allele is also associated with an increased risk of age-related cognitive decline during normal aging. Together, these findings suggest that the effect of the APOE4 genotype on cognitive deficits might due to inherent defects in synaptic function, that appeared before age-dependent markers of neuropathology and may be an independent risk factor affecting cognitive function.

In order to explore the contribution of different APOE isoforms to AD pathogenesis, it will be critical to investigate the molecular interactions that occur between APOE genotype and the its interacting molecules. To avoid the effects of endogenous APOE, and to exclude the confounding influence of secreted factors produced by glia, primary neurons from *APOE*$^{-/-}$ mice were selected and Co-IP/MS approach was used to screening the differently interactors of recombinant human APOE genotype. As the APOE4 allele conferring an increased risk relative to the most common APOE3 allele, so the recombinant human APOE3 was used as a standard APOE isoform. We identified a set of genes that differently bind to APOE3 and APOE4. The GO and KEGG analyses revealed that many of the proteins identified were linked to neurological disorders, such as AD, PD and Huntington diseases. The top rank difference between APOE4 and APOE3 specific interactome was enriched in SNARE interactions in vesicular transport and synaptic vesicle cycle. Noteworthy, the VAMP2 protein, one of the individual SNARE complexes, is the one of the top APOE4 interactors. Because the SNARE protein was recognized as the core component of the

protein machinery that facilitates the fusion of synaptic vesicles with the presynaptic terminals, which may suggest that APOE4 is likely involved in regulating synaptic vesicle fusion and the inhibiting release of neurotransmitters, and the SNARE protein might be a critical candidate responsible for APOE4 related cognitive decline. Indeed, our Co-IP and BiFC combined with PLA assay demonstrated that APOE directly interacts with VAMP2 proteins with E4 > E3 manner. In addition, molecular docking and MD simulation approaches suggested that the APOE4-VAMP2 interaction was more stable and has stronger affinity than that of APOE3, which further supported our results. As the single amino acid polymorphisms substantially alter the structure and function of APOE protein, the amino acid conformation near 112 position of APOE protein was analyzed. Detailed analysis suggest that higher free binding energy may be attributed to the increased hydrogen bonding between the APOE4 and VAMP2 protein. In neuronal cells, syntaxin-1 associates with SNAP25 to form t-SNARE complex in the presynaptic plasma membrane, which then assemble into full SNARE complex with VAMP2 on synaptic vesicles to mediate vesicles fusion with the membrane and neurotransmission[53]. The SNARE complex formation process implies that interactors that bind to the SNARE monomer are likely to affect the SNARE complex's formation (33, 38). Of note, the MDS assay suggests that interactions of APOE4 with VAMP2 may hamper the SNARE complex formation by blocking the VAMP2 binding interface. Studies reported that the SNARE-complex formation deficits might generally occur in cognitive impairment-related diseases, such as AD, PD, depression, and others (37, 38, 53). Deficits in SNARE complex assembly could inhibit neurotransmission and subsequently contribute to cognitive damage and disease pathology(54, 55). In addition, the formation of neuronal SNARE complex has been reported as a major target for modulation of various neural activities, and maintaining the SNARE protein function in neurotransmission was demonstrated important for preventing the neurodegeneration[33, 54-56]. Consistently, our present study showed that the SNARE complex formation was significantly decreased in AD mouse model compared to the age-matched wild types.

After demonstrating the interaction of APOE and VAMP2, we try to come up with original ideas as to whether they may affect the SNARE complex formation. Overexpression experiments *in vitro and in vivo* have shown that APOE4 can significantly directly inhibit the formation of SNARE complex. So, does this happen under physiological condition? To address this need, we employed a model of human APOE-TR mice, in which the mouse express human APOE alleles under the mouse APOE promoter, and do not develop the plaques and tangles diagnostic of AD[57]. APOE4-TR mice displayed a significant decrease in SNARE complex formation when compared with that of APOE3-TR mice, which in agreement with the overexpression results. Because APOE4-TR mice are specifically replacement mouse APOE gene with human APOE protein isoform, our in vivo data establishes a possible connection between APOE genotype and SNARE proteins. For no neuropathological features in APOE-TR mice, the results suggest that APOE4 may be an independent factor hinder the SNARE complex formation. Together, we demonstrated that APOE4 directly inhibit the formation of SNARE complex *in vitro and in vivo*.

Since we demonstrate that APOE4 can inhibit the formation of SNARE complex, and at synapses each exocytosis event dependent on the assembly of the SNARE complex, the effect of APOE4 on synapse exocytosis was monitored. Previous work performed in neurons and neurosecretory cells showed that

application of FM4-64 during periods of activity results in the labelling of recycling vesicles, which internalize the dye during exo-endocytosis processes[58]. Our in vitro experiments showed that the cells infection with AV-APOE4 led to more synaptic vesicle retention at presynaptic synaptosomes. Results suggested that APOE4 could obviously impair the synapse exocytosis. Furthermore, electron microscopy was used to assessed the synapse ultrastructure in APOE-TR mice. Results showed that compared to APOE3 neurons, APOE4 neurons had similar synaptic vesicles number, synaptic morphology, and active zone length, while with less numbers of docked synaptic vesicles at the active zone, which is the necessary step prior to membrane fusion. Collectively, our results are in coherence with previous studies suggesting that APOE4 is responsible for decreased neurotransmission and cognitive impairments and further identifies the underlying molecular mechanisms.

APOE4 contributes to AD pathogenesis through several overlapping cellular and molecular processes, including Aβ pathology, tau phosphorylation，mitochondrial dysfunction, dysregulated glucose metabolism, neuroinflammation dysregulation, synaptic damage, and neurotoxicity(61). In the present study, we raised the primary mechanism by which APOE4 affects cognitive decline. We believe that APOE4 directly hamper the SNARE complex formation, disrupts synaptic transmission, and trigger the downstream toxic pathways leading to cognitive deficits. This effect may be independent of any neuropathological changes. We believe that this mechanism is an essential complement to APOE4-induced neurodegenerative disease.

Our observations may have implications beyond AD. APOE4 is not only the strongest genetic susceptibility factor for AD, but also reported have an impact on a wide range of neurological disorders, such as frontotemporal dementia, Parkinson disease and Lewy body dementia[13-16]. It is worth noting that dysfunction of SNARE complex is a common phenomenon in these neurodegenerative disorders[37, 59, 60]. Therefore, our results altogether might suggest that APOE4 inhibition of SNARE complex formation is likely to be a shared pathogenic mechanism of APOE4 leading to neurodegeneration. Gaining a better understanding on the mechanisms of APOE-regulated SNARE complex formation should enhance our understanding about why APOE4 is a strong risk factor for cognitive decline and teach us about how we can target APOE in an isoform-specific manner to improve synaptic function to treat neurodegenerative diseases.

Although our study has shown that APOE4 directly interact with SNARE protein, affecting SNARE complex synthesis, and may be a potential pathogenesis mechanism of APOE4 mediated synaptic toxicity. While, several drawbacks need to be acknowledged. Firstly, since SNARE complex and associated proteins play a critical role in synaptic release, which involve several successive steps including vesicle docking, priming and fusion[61], we do not know the exact step in which APOE4 specific interacts with SNARE proteins to affect synaptic release. Secondly, we could not establish a causal relationship between APOE4-induced AD risk and SNARE complex formation, because APOE4 also has other toxic effects, such as Calcium homeostasis and blood-brain barrier (BBB) dysfunction, dysregulation of neuroinflammation and lipid transport, which were reported correlated with cognitive disorder[21, 62-64]. More work is needed to establish causality relationship. In addition, it is not clear whether APOE4 affects the SNARE complex

independently of other hallmark pathologies of AD, as APOE4 can affect these pathologic markers, and the pathologic markers such as Aβ can also affect the SNARE complex formation. Further studies are necessary to determine if those are causatively or consequently involved in neurodegeneration.

Conclusions

Collectively, our findings identify SNARE protein as a novel APOE interactor, the APOE4 isoform effects on SNARE complex formation then contributed to the APOE4-induced synaptic dysfunction. This report is in coherence with previous studies suggesting that APOE4 are the pathogens responsible for cognitive impairment in AD and further identify the underlying molecular mechanisms and the target protein machinery. Our findings provide new insights into the molecular mechanisms responsible for the susceptibility gene APOE, providing mechanistic insights for neurotransmitter exocytosis-based neurodegenerative diseases prevention and therapy.

List Of Abbreviations

AAV: adeno-associated virus

Aβ: amyloid-β

AD: Alzheimer's disease

APOE: Apolipoprotein E

AV: adenovirus

BBB: blood-brain barrier

BiFC: biomolecular fluorescence complementation

CNS: central nervous system

Co-IP: co-immunoprecipitation

GFP: green fluorescent protein

MDS: molecular dynamic simulations

MS: mass spectrometry

PLA: proximity ligation assay

RMSD: root-mean-square deviation

SNARE: soluble N-ethylmaleimide-sensitive factor attachment protein receptor

TEM: transmission electron microscopy

TG: transgenic

TR: targeted replacement

Declarations

Ethics approval and consent to participate:
All animal experimental procedures were performed in accordance with the Guide for the Care and Use of Laboratory Animals and approved by the Laboratory Animal Ethical Committee of Guangdong Medical University.
Consent for publication:
Not applicable.
Availability of data and materials:
All data needed to evaluate the conclusions in the paper are present in the paper and/or the Supplementary Materials. Additional data related to this paper may be requested from the authors
Competing interests:
The authors declare that they have no conflict of interest.
Funding:
This work was supported by National Natural Science Foundation of China (82071190); Guangdong Province Universities and Colleges Pearl River Scholar Funded Scheme (2017) and Foundation for High-level Talents in Higher Education of Guangdong (2016) to L.C.
Acknowledgements:
Not applicable
Author information:
Affiliations
Guangdong Key Laboratory of Age-Related Cardiac and Cerebral Diseases, Affiliated Hospital of Guangdong Medical University, Zhanjiang, China.
Feng Chen, Yanting Chen, Huiyi Chen, Yongxiang Wang, Yujie Cai, Chunmei Liang, Xiongjin Chen, Yao Ji, Yan Wang, Lili Cui
Department of Neurology, Affiliated Hospital of Guangdong Medical University, Zhanjiang, China.
Yanting Chen, Huiyi Chen, Yongxiang Wang, Yao Ji
Department of gerontology, Affiliated Hospital of Guangdong Medical University, Zhanjiang, China.
Wenyan Wei
School of Life Science and Biopharmaceutics, Shenyang Pharmaceutical University, 103 Wenhua Road, Shenyang, China.
Hao Cao
Department of Psychiatry, Guangdong Key Laboratory of Age-Related Cardiac and Cerebral Diseases, Affiliated Hospital of Guangdong Medical University, Zhanjiang, China.
Dandan Zhang

Department of Pharmacology and Neuroscience, University of North Texas Health Science Center, Fort Worth, TX, USA.
Yuanhong Sun
Contributions:
The study was designed by L.C. and Y.W. (Yan Wang) and performed by F.C., Y.C., H.C., Y.W. (Yongxiang Wang), W.W., Y.C., C.L., X.C., Y.J. and H.C. Results were analyzed by F.C., Y.C., Y.S., D.Z. and H.C. The molecular dynamic simulations were conducted by H.C. The manuscript was original drafted by F.C. and revised by L.C. and Y.W. (Yan Wang). All authors approved the final version of manuscript.

Reference

1. Lambert JC, Ibrahim-Verbaas CA, Harold D, Naj AC, Sims R, Bellenguez C, DeStafano AL, Bis JC, Beecham GW, Grenier-Boley B, et al: **Meta-analysis of 74,046 individuals identifies 11 new susceptibility loci for Alzheimer's disease.***Nat Genet* 2013, **45:**1452-1458.
2. Scheltens P, Blennow K, Breteler MM, de Strooper B, Frisoni GB, Salloway S, Van der Flier WM: **Alzheimer's disease.***Lancet* 2016, **388:**505-517.
3. Selkoe DJ: **Alzheimer's disease is a synaptic failure.***Science* 2002, **298:**789-791.
4. DeKosky ST, Scheff SW: **Synapse loss in frontal cortex biopsies in Alzheimer's disease: correlation with cognitive severity.***Ann Neurol* 1990, **27:**457-464.
5. Masliah E, Mallory M, Alford M, DeTeresa R, Hansen LA, McKeel DW, Jr., Morris JC: **Altered expression of synaptic proteins occurs early during progression of Alzheimer's disease.***Neurology* 2001, **56:**127-129.
6. Terry RD, Masliah E, Salmon DP, Butters N, DeTeresa R, Hill R, Hansen LA, Katzman R: **Physical basis of cognitive alterations in Alzheimer's disease: synapse loss is the major correlate of cognitive impairment.***Ann Neurol* 1991, **30:**572-580.
7. Ramos-Miguel A, Sawada K, Jones AA, Thornton AE, Barr AM, Leurgans SE, Schneider JA, Bennett DA, Honer WG: **Presynaptic proteins complexin-I and complexin-II differentially influence cognitive function in early and late stages of Alzheimer's disease.***Acta Neuropathol* 2017, **133:**395-407.
8. McInnes J, Wierda K, Snellinx A, Bounti L, Wang YC, Stancu IC, Apostolo N, Gevaert K, Dewachter I, Spires-Jones TL, et al: **Synaptogyrin-3 Mediates Presynaptic Dysfunction Induced by Tau.***Neuron* 2018, **97:**823-835 e828.
9. Yamazaki Y, Zhao N, Caulfield TR, Liu CC, Bu G: **Apolipoprotein E and Alzheimer disease: pathobiology and targeting strategies.***Nat Rev Neurol* 2019, **15:**501-518.
10. van der Lee SJ, Wolters FJ, Ikram MK, Hofman A, Ikram MA, Amin N, van Duijn CM: **The effect of APOE and other common genetic variants on the onset of Alzheimer's disease and dementia: a community-based cohort study.***Lancet Neurol* 2018, **17:**434-444.
11. Corder EH, Saunders AM, Strittmatter WJ, Schmechel DE, Gaskell PC, Small GW, Roses AD, Haines JL, Pericak-Vance MA: **Gene dose of apolipoprotein E type 4 allele and the risk of Alzheimer's disease in**

late onset families.*Science* 1993, **261:**921-923.

12. Neu SC, Pa J, Kukull W, Beekly D, Kuzma A, Gangadharan P, Wang LS, Romero K, Arneric SP, Redolfi A, et al: **Apolipoprotein E Genotype and Sex Risk Factors for Alzheimer Disease: A Meta-analysis.***JAMA Neurol* 2017, **74:**1178-1189.
13. Tsuang D, Leverenz JB, Lopez OL, Hamilton RL, Bennett DA, Schneider JA, Buchman AS, Larson EB, Crane PK, Kaye JA, et al: **APOE epsilon4 increases risk for dementia in pure synucleinopathies.***JAMA Neurol* 2013, **70:**223-228.
14. Davis AA, Inman CE, Wargel ZM, Dube U, Freeberg BM, Galluppi A, Haines JN, Dhavale DD, Miller R, Choudhury FA, et al: **APOE genotype regulates pathology and disease progression in synucleinopathy.***Sci Transl Med* 2020, **12**.
15. Mishra A, Ferrari R, Heutink P, Hardy J, Pijnenburg Y, Posthuma D, International FTDGC: **Gene-based association studies report genetic links for clinical subtypes of frontotemporal dementia.***Brain* 2017, **140:**1437-1446.
16. Zhao N, Attrebi ON, Ren Y, Qiao W, Sonustun B, Martens YA, Meneses AD, Li F, Shue F, Zheng J, et al: **APOE4 exacerbates alpha-synuclein pathology and related toxicity independent of amyloid.***Sci Transl Med* 2020, **12**.
17. Hatters DM, Peters-Libeu CA, Weisgraber KH: **Apolipoprotein E structure: insights into function.***Trends Biochem Sci* 2006, **31:**445-454.
18. Holtzman DM, Herz J, Bu G: **Apolipoprotein E and apolipoprotein E receptors: normal biology and roles in Alzheimer disease.***Cold Spring Harb Perspect Med* 2012, **2:**a006312.
19. Frieden C, Garai K: **Structural differences between apoE3 and apoE4 may be useful in developing therapeutic agents for Alzheimer's disease.***Proc Natl Acad Sci U S A* 2012, **109:**8913-8918.
20. LaDu MJ, Falduto MT, Manelli AM, Reardon CA, Getz GS, Frail DE: **Isoform-specific binding of apolipoprotein E to beta-amyloid.***J Biol Chem* 1994, **269:**23403-23406.
21. Shi Y, Holtzman DM: **Interplay between innate immunity and Alzheimer disease: APOE and TREM2 in the spotlight.***Nat Rev Immunol* 2018, **18:**759-772.
22. Lane-Donovan C, Herz J: **ApoE, ApoE Receptors, and the Synapse in Alzheimer's Disease.***Trends Endocrinol Metab* 2017, **28:**273-284.
23. Yu JT, Tan L, Hardy J: **Apolipoprotein E in Alzheimer's disease: an update.***Annu Rev Neurosci* 2014, **37:**79-100.
24. Arendt T, Schindler C, Bruckner MK, Eschrich K, Bigl V, Zedlick D, Marcova L: **Plastic neuronal remodeling is impaired in patients with Alzheimer's disease carrying apolipoprotein epsilon 4 allele.***J Neurosci* 1997, **17:**516-529.
25. Ji Y, Gong Y, Gan W, Beach T, Holtzman DM, Wisniewski T: **Apolipoprotein E isoform-specific regulation of dendritic spine morphology in apolipoprotein E transgenic mice and Alzheimer's disease patients.***Neuroscience* 2003, **122:**305-315.

26. Wang C, Wilson WA, Moore SD, Mace BE, Maeda N, Schmechel DE, Sullivan PM: **Human apoE4-targeted replacement mice display synaptic deficits in the absence of neuropathology.***Neurobiol Dis* 2005, **18:**390-398.
27. Klein RC, Mace BE, Moore SD, Sullivan PM: **Progressive loss of synaptic integrity in human apolipoprotein E4 targeted replacement mice and attenuation by apolipoprotein E2.***Neuroscience* 2010, **171:**1265-1272.
28. Bao H, Das D, Courtney NA, Jiang Y, Briguglio JS, Lou X, Roston D, Cui Q, Chanda B, Chapman ER: **Dynamics and number of trans-SNARE complexes determine nascent fusion pore properties.***Nature* 2018, **554:**260-263.
29. Zhou Q, Lai Y, Bacaj T, Zhao M, Lyubimov AY, Uervirojnangkoorn M, Zeldin OB, Brewster AS, Sauter NK, Cohen AE, et al: **Architecture of the synaptotagmin-SNARE machinery for neuronal exocytosis.***Nature* 2015, **525:**62-67.
30. Sudhof TC, Rothman JE: **Membrane fusion: grappling with SNARE and SM proteins.***Science* 2009, **323:**474-477.
31. Corradini I, Verderio C, Sala M, Wilson MC, Matteoli M: **SNAP-25 in neuropsychiatric disorders.***Ann N Y Acad Sci* 2009, **1152:**93-99.
32. Honer WG, Falkai P, Bayer TA, Xie J, Hu L, Li HY, Arango V, Mann JJ, Dwork AJ, Trimble WS: **Abnormalities of SNARE mechanism proteins in anterior frontal cortex in severe mental illness.***Cereb Cortex* 2002, **12:**349-356.
33. Burre J, Sharma M, Tsetsenis T, Buchman V, Etherton MR, Sudhof TC: **Alpha-synuclein promotes SNARE-complex assembly in vivo and in vitro.***Science* 2010, **329:**1663-1667.
34. Choi BK, Choi MG, Kim JY, Yang Y, Lai Y, Kweon DH, Lee NK, Shin YK: **Large alpha-synuclein oligomers inhibit neuronal SNARE-mediated vesicle docking.***Proc Natl Acad Sci U S A* 2013, **110:**4087-4092.
35. Ramos-Miguel A, Jones AA, Sawada K, Barr AM, Bayer TA, Falkai P, Leurgans SE, Schneider JA, Bennett DA, Honer WG: **Frontotemporal dysregulation of the SNARE protein interactome is associated with faster cognitive decline in old age.***Neurobiol Dis* 2018, **114:**31-44.
36. Honer WG, Barr AM, Sawada K, Thornton AE, Morris MC, Leurgans SE, Schneider JA, Bennett DA: **Cognitive reserve, presynaptic proteins and dementia in the elderly.***Transl Psychiatry* 2012, **2:**e114.
37. Sharma M, Burre J, Sudhof TC: **Proteasome inhibition alleviates SNARE-dependent neurodegeneration.***Sci Transl Med* 2012, **4:**147ra113.
38. Yang Y, Kim J, Kim HY, Ryoo N, Lee S, Kim Y, Rhim H, Shin YK: **Amyloid-beta Oligomers May Impair SNARE-Mediated Exocytosis by Direct Binding to Syntaxin 1a.***Cell Rep* 2015, **12:**1244-1251.
39. Wang Y, Yang JQ, Hong TT, Sun YH, Huang HL, Chen F, Chen XJ, Chen HY, Dong SS, Cui LL, Yang TL: **RTN4B-mediated suppression of Sirtuin 2 activity ameliorates beta-amyloid pathology and cognitive impairment in Alzheimer's disease mouse model.***Aging Cell* 2020, **19:**e13194.
40. Strittmatter WJ, Saunders AM, Goedert M, Weisgraber KH, Dong LM, Jakes R, Huang DY, Pericak-Vance M, Schmechel D, Roses AD: **Isoform-specific interactions of apolipoprotein E with microtubule-**

associated protein tau: implications for Alzheimer disease.*Proc Natl Acad Sci U S A* 1994, **91:**11183-11186.

41. Koo SJ, Kochlamazashvili G, Rost B, Puchkov D, Gimber N, Lehmann M, Tadeus G, Schmoranzer J, Rosenmund C, Haucke V, Maritzen T: **Vesicular Synaptobrevin/VAMP2 Levels Guarded by AP180 Control Efficient Neurotransmission.***Neuron* 2015, **88:**330-344.
42. Di Giovanni J, Boudkkazi S, Mochida S, Bialowas A, Samari N, Leveque C, Youssouf F, Brechet A, Iborra C, Maulet Y, et al: **V-ATPase membrane sector associates with synaptobrevin to modulate neurotransmitter release.***Neuron* 2010, **67:**268-279.
43. Drummond E, Pires G, MacMurray C, Askenazi M, Nayak S, Bourdon M, Safar J, Ueberheide B, Wisniewski T: **Phosphorylated tau interactome in the human Alzheimer's disease brain.***Brain* 2020.
44. Sharda N, Pengo T, Wang Z, Kandimalla KK: **Amyloid-beta Peptides Disrupt Interactions Between VAMP-2 and SNAP-25 in Neuronal Cells as Determined by FRET/FLIM.***J Alzheimers Dis* 2020, **77:**423-435.
45. Shin JH, Park SJ, Jo DS, Park NY, Kim JB, Bae JE, Jo YK, Hwang JJ, Lee JA, Jo DG, et al: **Down-regulated TMED10 in Alzheimer disease induces autophagy via ATG4B activation.***Autophagy* 2019, **15:**1495-1505.
46. Sun X, Dong C, Levin B, Crocco E, Loewenstein D, Zetterberg H, Blennow K, Wright CB, Alzheimer's Disease Neuroimaging I: **APOE epsilon4 carriers may undergo synaptic damage conferring risk of Alzheimer's disease.***Alzheimers Dement* 2016, **12:**1159-1166.
47. Asaro A, Carlo-Spiewok AS, Malik AR, Rothe M, Schipke CG, Peters O, Heeren J, Willnow TE: **Apolipoprotein E4 disrupts the neuroprotective action of sortilin in neuronal lipid metabolism and endocannabinoid signaling.***Alzheimers Dement* 2020, **16:**1248-1258.
48. Caselli RJ, Dueck AC, Osborne D, Sabbagh MN, Connor DJ, Ahern GL, Baxter LC, Rapcsak SZ, Shi J, Woodruff BK, et al: **Longitudinal modeling of age-related memory decline and the APOE epsilon4 effect.***N Engl J Med* 2009, **361:**255-263.
49. Buttini M, Orth M, Bellosta S, Akeefe H, Pitas RE, Wyss-Coray T, Mucke L, Mahley RW: **Expression of human apolipoprotein E3 or E4 in the brains of Apoe-/- mice: isoform-specific effects on neurodegeneration.***J Neurosci* 1999, **19:**4867-4880.
50. Dik MG, Jonker C, Comijs HC, Bouter LM, Twisk JW, van Kamp GJ, Deeg DJ: **Memory complaints and APOE-epsilon4 accelerate cognitive decline in cognitively normal elderly.***Neurology* 2001, **57:**2217-2222.
51. Reiman EM, Chen K, Alexander GE, Caselli RJ, Bandy D, Osborne D, Saunders AM, Hardy J: **Functional brain abnormalities in young adults at genetic risk for late-onset Alzheimer's dementia.***Proc Natl Acad Sci U S A* 2004, **101:**284-289.
52. Trommer BL, Shah C, Yun SH, Gamkrelidze G, Pasternak ES, Ye GL, Sotak M, Sullivan PM, Pasternak JF, LaDu MJ: **ApoE isoform affects LTP in human targeted replacement mice.***Neuroreport* 2004, **15:**2655-2658.
53. Rizo J, Xu J: **The Synaptic Vesicle Release Machinery.***Annu Rev Biophys* 2015, **44:**339-367.

54. Sharma M, Burre J, Sudhof TC: **CSPalpha promotes SNARE-complex assembly by chaperoning SNAP-25 during synaptic activity.***Nat Cell Biol* 2011, **13:**30-39.
55. Haberman A, Williamson WR, Epstein D, Wang D, Rina S, Meinertzhagen IA, Hiesinger PR: **The synaptic vesicle SNARE neuronal Synaptobrevin promotes endolysosomal degradation and prevents neurodegeneration.***J Cell Biol* 2012, **196:**261-276.
56. Burgoyne RD, Morgan A: **Cysteine string protein (CSP) and its role in preventing neurodegeneration.***Semin Cell Dev Biol* 2015, **40:**153-159.
57. Sullivan PM, Mezdour H, Aratani Y, Knouff C, Najib J, Reddick RL, Quarfordt SH, Maeda N: **Targeted replacement of the mouse apolipoprotein E gene with the common human APOE3 allele enhances diet-induced hypercholesterolemia and atherosclerosis.***J Biol Chem* 1997, **272:**17972-17980.
58. Gaffield MA, Betz WJ: **Imaging synaptic vesicle exocytosis and endocytosis with FM dyes.***Nat Protoc* 2006, **1:**2916-2921.
59. Costa AS, Guerini FR, Arosio B, Galimberti D, Zanzottera M, Bianchi A, Nemni R, Clerici M: **SNARE Complex Polymorphisms Associate with Alterations of Visual Selective Attention in Alzheimer's Disease.***J Alzheimers Dis* 2019, **69:**179-188.
60. Agliardi C, Meloni M, Guerini FR, Zanzottera M, Bolognesi E, Baglio F, Clerici M: **Oligomeric alpha-Syn and SNARE complex proteins in peripheral extracellular vesicles of neural origin are biomarkers for Parkinson's disease.***Neurobiol Dis* 2020, **148:**105185.
61. Sudhof TC: **Neurotransmitter release: the last millisecond in the life of a synaptic vesicle.***Neuron* 2013, **80:**675-690.
62. Montagne A, Nation DA, Sagare AP, Barisano G, Sweeney MD, Chakhoyan A, Pachicano M, Joe E, Nelson AR, D'Orazio LM, et al: **APOE4 leads to blood-brain barrier dysfunction predicting cognitive decline.***Nature* 2020, **581:**71-76.
63. Ioannou MS, Jackson J, Sheu SH, Chang CL, Weigel AV, Liu H, Pasolli HA, Xu CS, Pang S, Matthies D, et al: **Neuron-Astrocyte Metabolic Coupling Protects against Activity-Induced Fatty Acid Toxicity.***Cell* 2019, **177:**1522-1535 e1514.
64. van Vliet P, Oleksik AM, Mooijaart SP, de Craen AJ, Westendorp RG: **APOE genotype modulates the effect of serum calcium levels on cognitive function in old age.***Neurology* 2009, **72:**821-828.

Figures

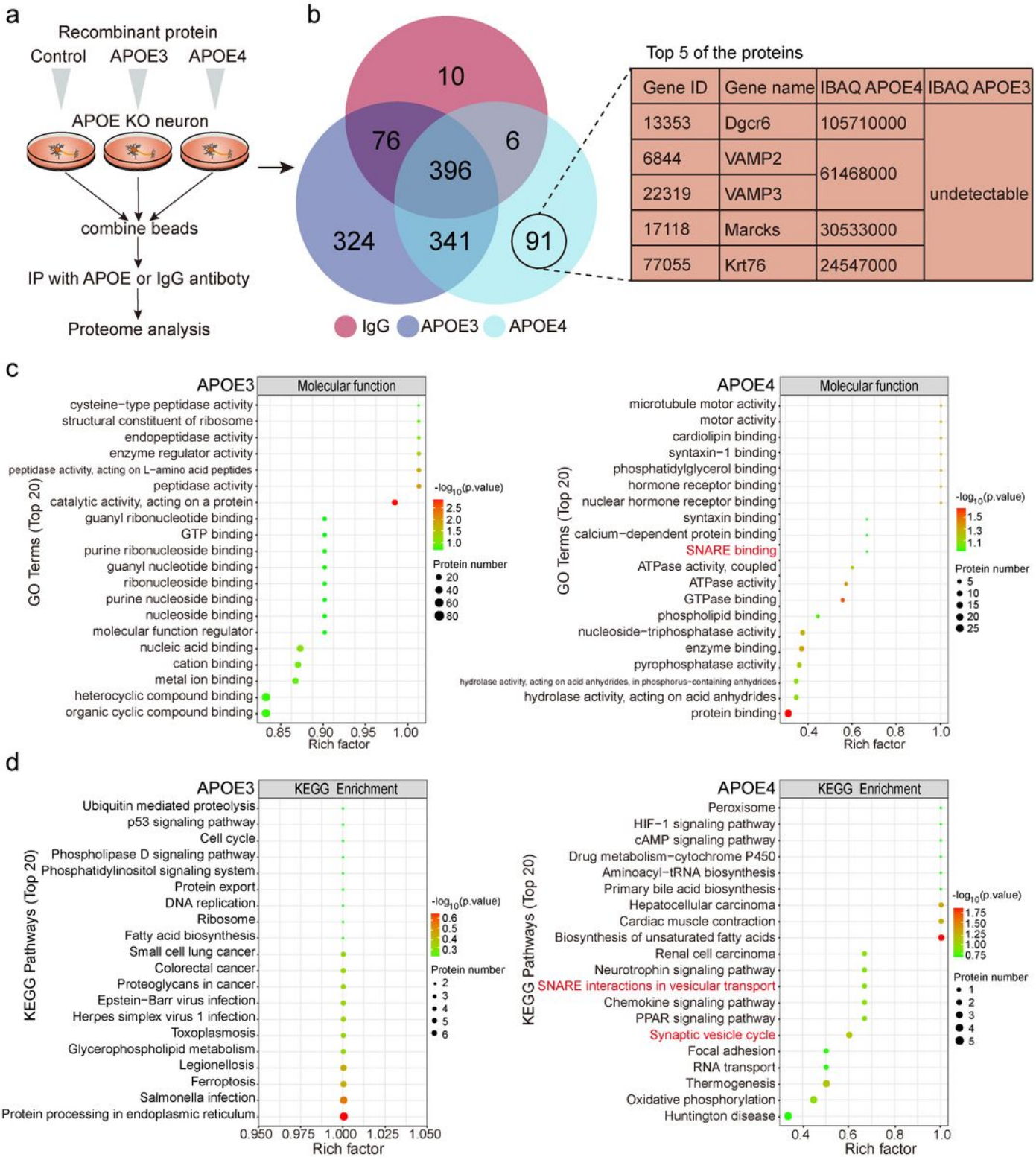

Figure 1

Characterization of different interactions of the APOE genotype in vitro. (A) Flow chart of the experimental approach to identify APOE genotype-dependent interacting proteins. APOE-/- primary neurons were incubated wsuppith either recombinant human APOE3 or APOE4 protein (10 μg/mL for 24 h), then Co-IP and MS analysis were performed to screen the potential APOE trapped proteins. IgG was used as negative control. (B) Venn-diagram depicting the number of interaction proteins among the

APOE3, APOE4, and IgG groups. The top five of the APOE4-specifically enriched proteins were listed according to the abundance in MS data. (C) GO term enrichment analysis (molecular function) of the APOE3 and APOE4-specifically interacting proteins (top 20). (D) KEGG pathway analysis of the APOE3 and APOE4-specifically enriched proteins were listed (top 20).

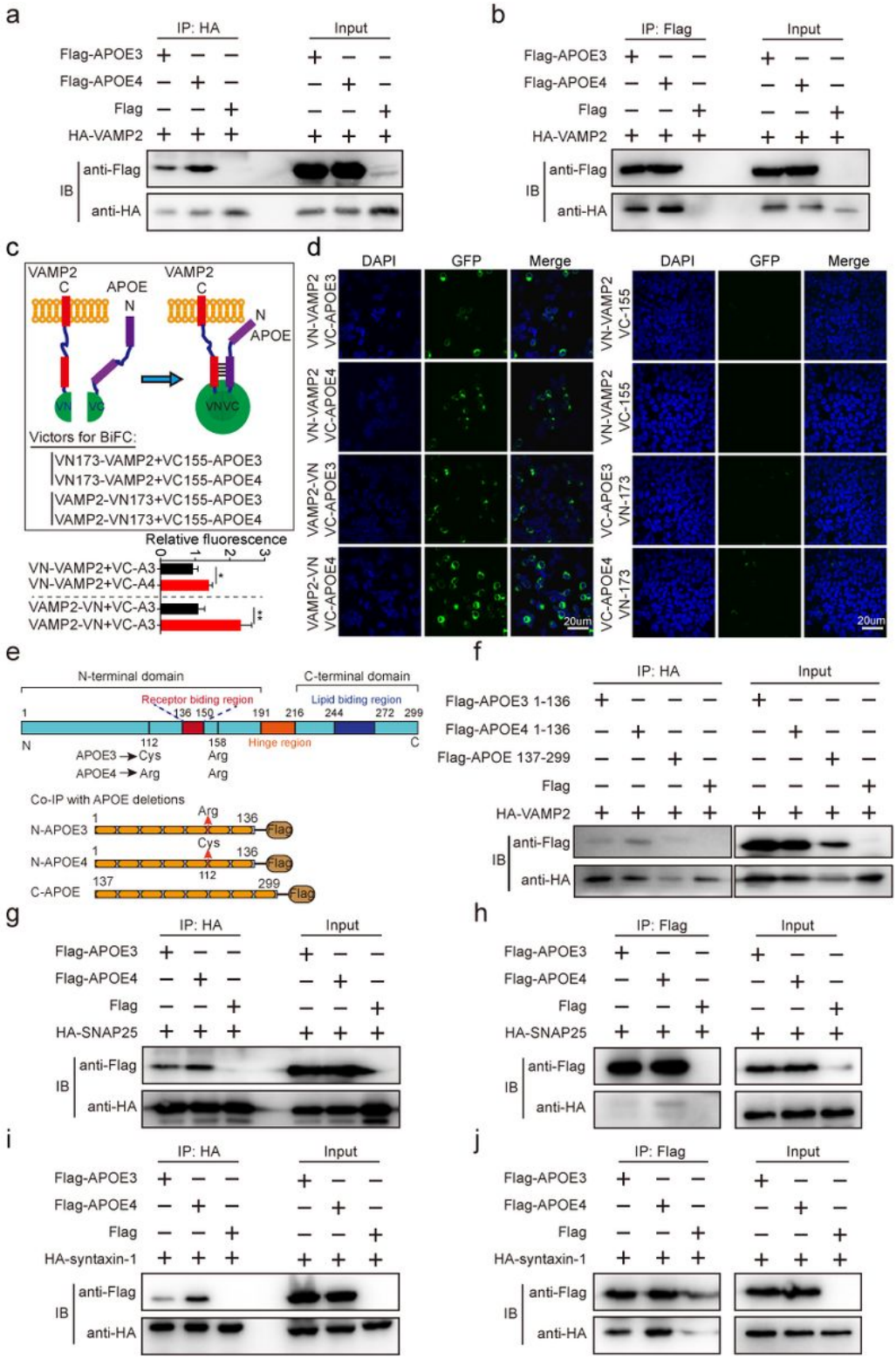

Figure 2

APOE interacts with SNARE proteins in an isoform-specific fashion (E4 > E3). (A–B) HA-VAMP2 and Flag-APOE (APOE3 or APOE4) plasmids were transiently co-transfected into HEK-293T cells. Cell lysates were immunoprecipitated by anti-HA or anti-Flag antibodies and subsequently immunoblotted with the indicated antibodies. (C) Principle of the BiFC assay. (D) BIFC analysis of the interaction between VAMP2 and APOE proteins. HEK-293T cells were transiently co-transfected with the BiFC plasmids, VN-VAMP2 and VC-APOE (APOE3 or APOE4), or VAMP2-VN and VC-APOE (APOE3 or APOE4) plasmids. After 48 h of transfection, the cells were imaged by fluorescence microscopy, and the relative fluorescence intensity of Venus was measured using a fluorescence microplate reader. (E) The APOE3 and APOE4 isoforms of APOE differ from one another at amino acid residues 112, APOE3 (Cys112) and APOE4 (Arg112). (F) HA-VAMP2 was co-transfected with Flag-APOE3 (1–136), Flag-APOE4 (1–136), or Flag-APOE (137–299) plasmids into HEK-293T cells. Cell lysates were subjected to immunoprecipitation and subsequent immunoblotting using the indicated antibodies. (G–J) HA-SNAP25 or HA-syntaxin-1 plasmids were transiently co-transfected with Flag-APOE (APOE3 or APOE4) plasmids in HEK-293T cells. Cell lysates were immunoprecipitated by anti-HA or Flag antibodies and subsequently immunoblotted with the indicated antibodies. one-way ANOVA was used to analyze the BiFC assay. Data are presented as mean ± SEM, *$p < 0.05$; **$p < 0.01$; ***$p < 0.001$. At least three independent experiments were performed.

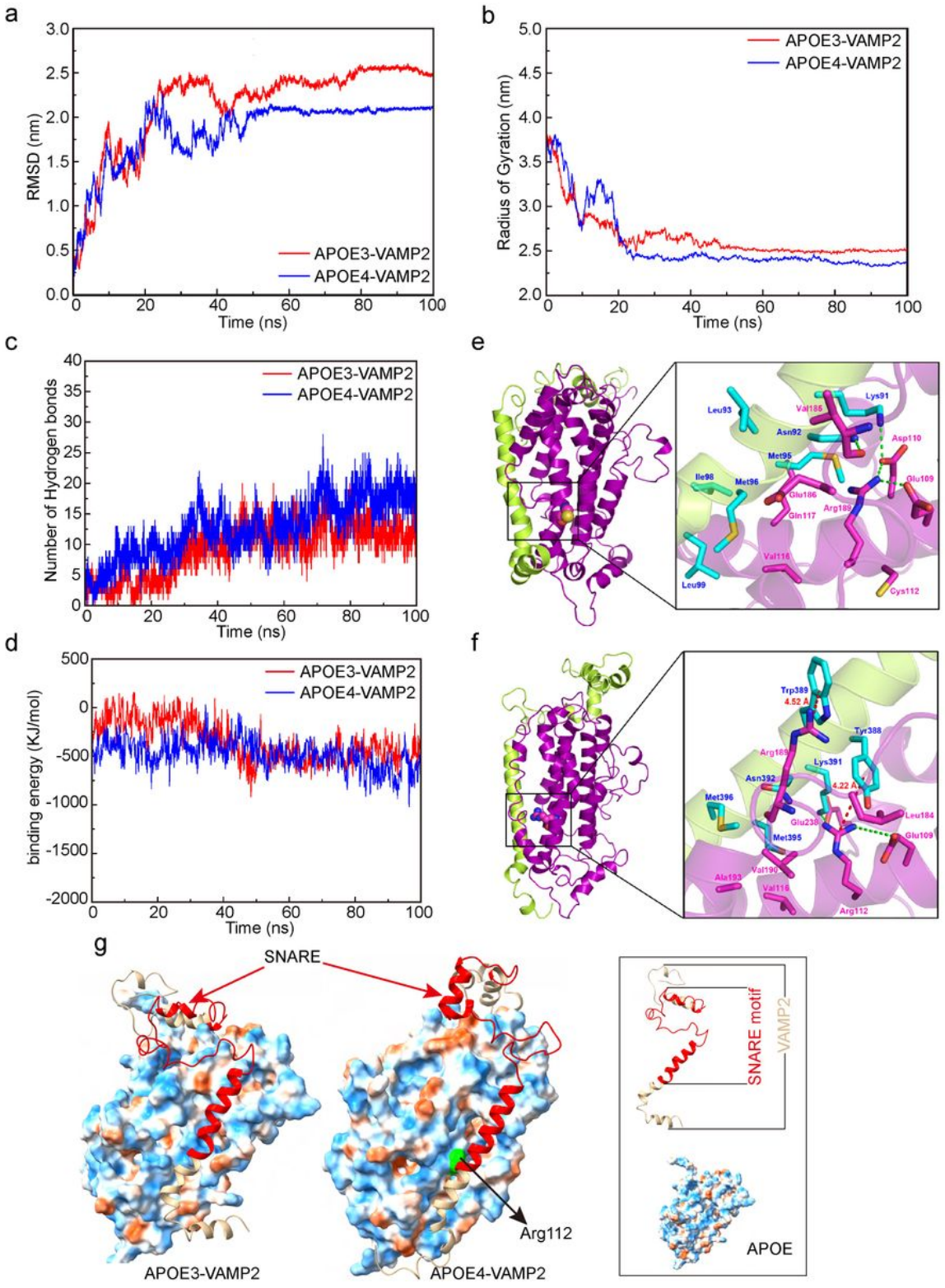

Figure 3

Molecular docking and molecular dynamics simulation. (A) Backbone RMSD of APOE3-VAMP2 and APOE4-VAMP2 complex with time at 300 K. The ordinate represents RMSD (nm), and the abscissa represents time (ns). (B) The protein structures compactness analysis by Rg of APOE3-VAMP2 and APOE4-VAMP2 complexes during 100 ns of MD simulation. The ordinate represents Rg (nm), and the abscissa represents time (ns). Changes in hydrogen bond number (C) and binding energy (D) between the

APOE protein and VAMP2 with MDS time. Color scheme: red indicates APOE3-VAMP2, blue indicates APOE3-VAMP2. (E, F) Differences in the binding of APOE3 and APOE4 with VAMP2. (G) The binding patterns of VAMP2 on APOE3 and APOE4 protein surfaces (cartoon model represents VAMP2; red region represents the region forming SNARE complex with SNAP25 and syntaxin-1 proteins; APOE3 and APOE4 are represented by surface model; blue and orange regions on protein surface represent hydrophilic and hydrophobic domains, respectively).

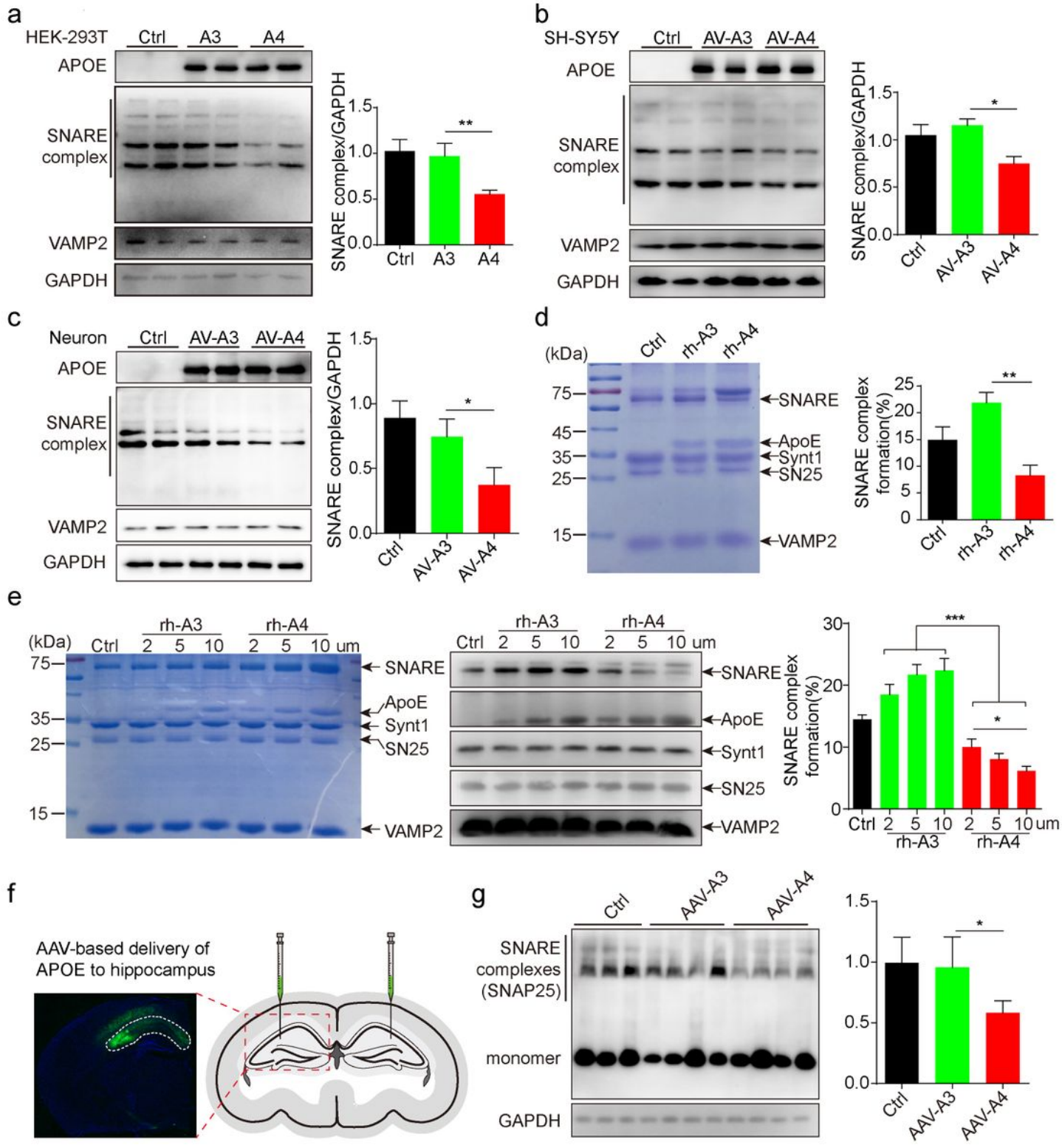

Figure 4

APOE4 effectively inhibits the formation of the SNARE complex in vitro and in vivo. (A) HEK-293T cells were co-transfected with constant amounts (1 μg/mL) of VAMP2, SNAP25, syntaxin-1, and APOE3 or APOE4 plasmid. Cell lysates were immunoblotted without boiling. The SNARE complex was determined by anti-VAMP2. The expression of the SNARE complex was normalized with the GAPDH protein. (B) SH-SY5Y cells were infected with adenovirus-mediated APOE3 and APOE4. SNARE complex levels were determined by western blot. (C) APOE-/- primary neurons were infected with adenovirus-mediated APOE3 and APOE4. SNARE complex levels were determined by western blot. (D) A Coomassie-stained gel showing a decrease in the amount of the SNARE complex assemble in the presence of APOE4 in a 20-min reaction. (E) Different doses of recombinant human APOE3 or APOE4 protein (2, 5, and 10 μM) on SNARE complex formation determined by Coomassie-stained gel. (F) The illustration of the bilateral hippocampal stereotactic injection and the infection efficiency of AAVs was assessed by immunofluorescence. (G) Expression levels of the SNARE complex were examined in the hippocampus of 7-month-old AAV (AAV-CMV-EGFP, AAV-APOE3, and AAV-APOE4)- injected female mice (n=6-8 mice per group). one-way ANOVA was used for (A-C, E and G), nonpaired Student's t test was used for D. Data are presented as mean ± SEM, *p < 0.05; **p < 0.01; ***p <0.001. At least three independent experiments were performed.

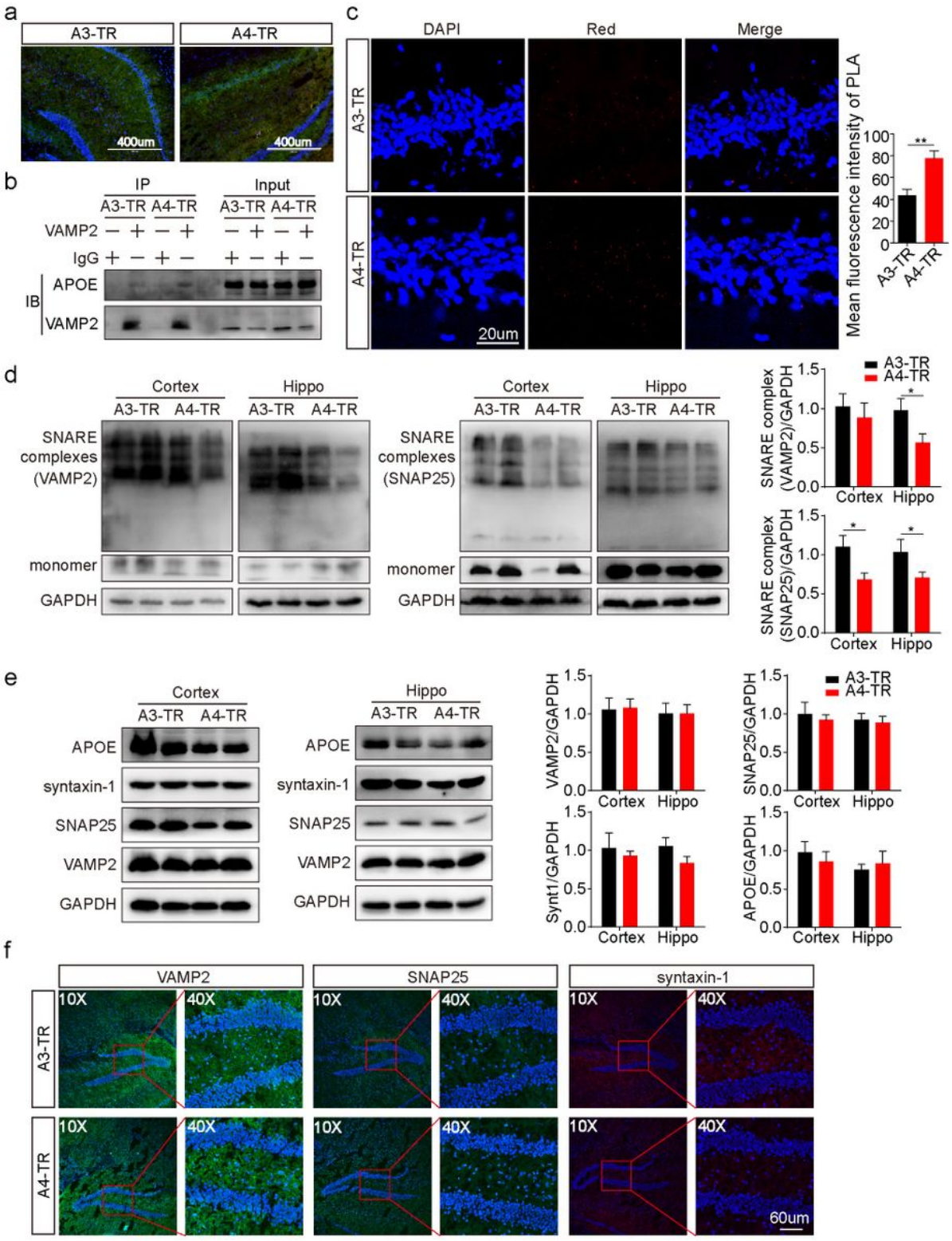

Figure 5

APOE4 decreases SNARE complex assembly under physiological conditions. (A) Endogenous APOE (red) and VAMP2 (green) were stained using relative antibodies in the hippocampal tissue from the APOE3- and APOE4-TR mice brain. (B) The lysates of the hippocampal tissue from APOE-TR mice were immunoprecipitated by anti-VAMP2 or anti-IgG antibodies and subsequently immunoblotted with the indicated antibodies. (C) The Duolink analysis verified that APOE4 has a higher interaction with VAMP2

than APOE3 in the hippocampus of APOE3- and APOE4-TR mice. The red particles represent interaction of APOE with VAMP2. (D) Expression levels of the SNARE complex were examined in the cortices and hippocampus of 6-month-old human APOE3 and APOE4-TR female mice (n=6 mice per group). (E) Relative expression of APOE, VAMP2, SNAP25, and syntaxin-1 in the cortices and hippocampus of 6-month-old human APOE3 and APOE4-TR female mice were determined by immunoblot (n=6 mice per group). (F) Representative images showing the fluorescence intensity of VAMP2, SNAP25, and syntaxin-1 in the hippocampus of APOE-TR mice by immunofluorescence staining of relative antibodies (n=4 mice per group). Quantification was performed according to the density of blot bands ratio to GAPDH. Data are presented as mean ± SEM, *p < 0.05. Data analyzed by one-way ANOVA. At least three independent experiments were performed.

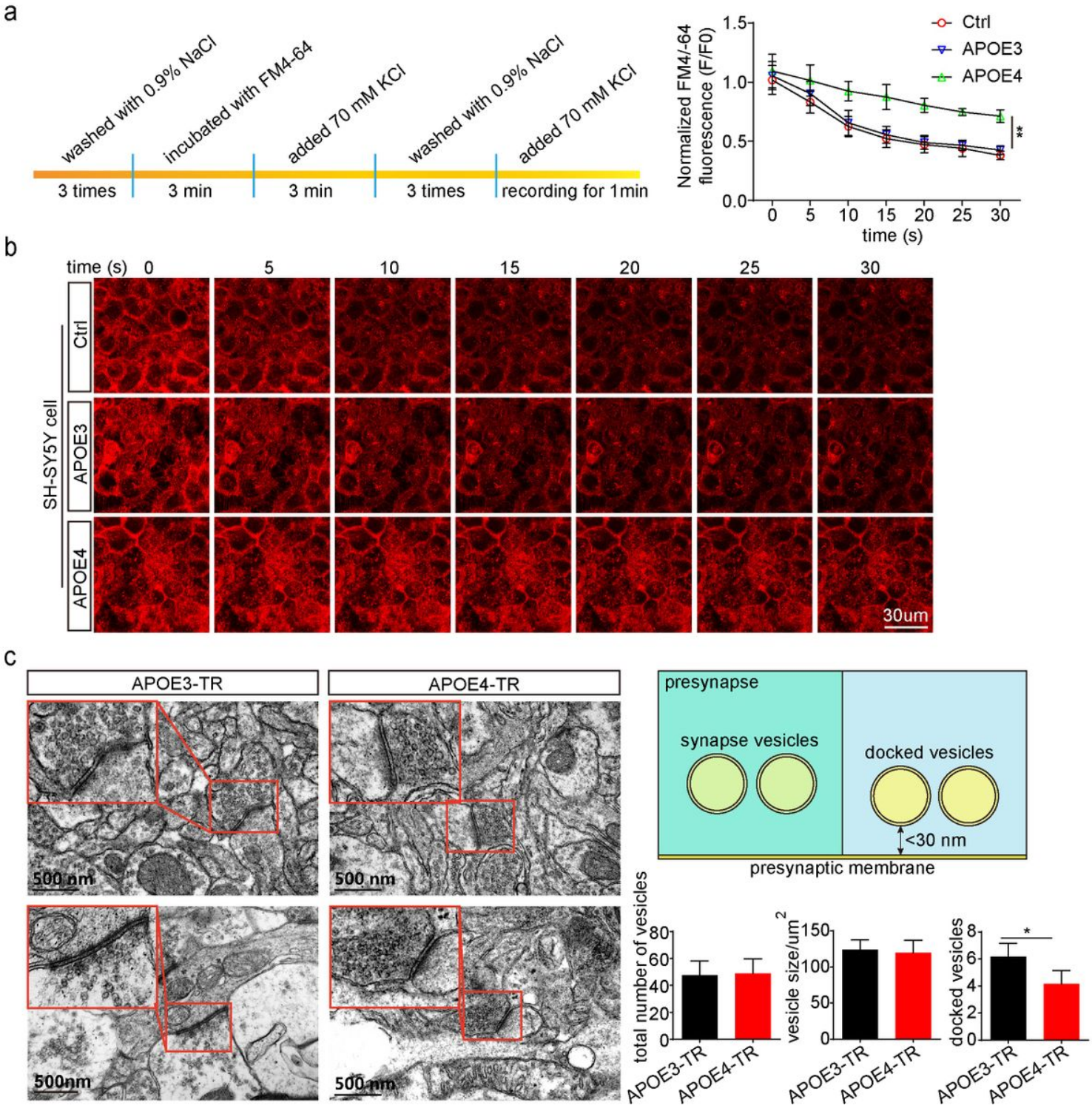

Figure 6

APOE4 is associated with decreased synaptic vesicle release. (A) Experimental protocol for FM4-64-loading and unloading. (B) Representative fluorescence intensity of SH-SY5Y cells stained with FM4-64 in each condition. SH-SY5Y cells were infected with adenovirus-mediated APOE3, APOE4, and control adenovirus for 48 h, then the cells were incubated with FM4-64 dye and treated with 70 mM KCl to label the synaptic vesicles. Next, 70 mM KCl was added to the FM4-64 loaded cells at room temperature to stimulate the exocytosis. Two-way ANOVA test was used to compare the exocytosis among different

groups. (C) TEM images from the CA1 region of the hippocampus from 7-month-old APOE3-TR and APOE4-TR mice. Docked vesicles were determined as located within 30 nm of the presynaptic active zone (n=5 mice per group). Data are presented as mean ± SEM, *p < 0.05; **p < 0.01; ***p < 0.001. Two-way ANOVA for (B), one-way ANOVA for (C). At least three independent experiments were performed.

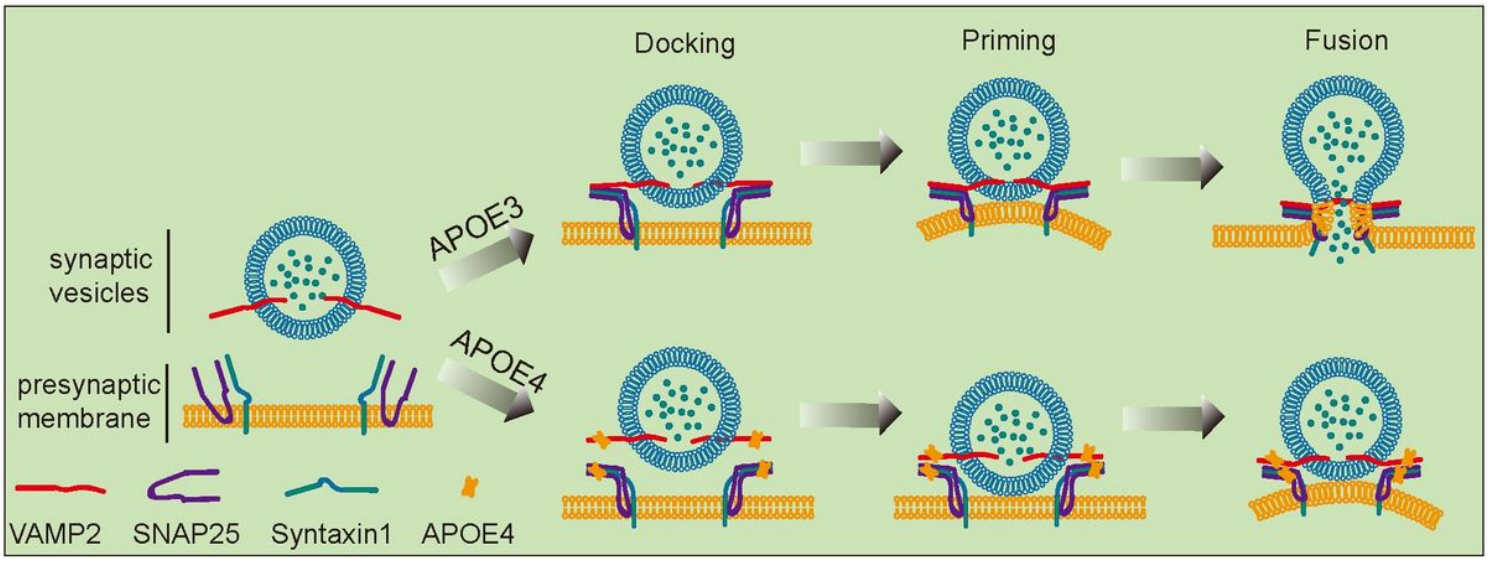

Figure 7

A mechanistic model shows that APOE4 inhibits the SNARE-mediated exocytosis. Normal SNARE-mediated exocytosis involves full zippering of the SNARE complex, which induces pore fusion. A hypothetical mechanistic model shows that APOE4 bind to v-SNAREs in such a way that impedes SNARE complex assembly, thereby inhibiting pore formation.

Supplementary Files

This is a list of supplementary files associated with this preprint. Click to download.

- renamed1c5a7.docx
- renamed49d84.mov
- renamed52128.tif
- renamed5b192.docx
- renamed5cd2f.mov
- renamed616d4.mov
- renamed80f8a.mov
- renamedab870.tif
- renamedb6ce5.tif
- renamedcf082.tif
- renamedda189.docx

- renamede592a.mov